

ALOS PALSAR interferometry in the Tien Shan: Detection of the Dec. 26, Kochkorka, Kyrgyzstan earthquake?

Robert Mellors⁽¹⁾, Arifandy Aulia⁽¹⁾, and David Sandwell⁽²⁾

⁽¹⁾ San Diego State University, Department of Geological Sciences, San Diego, CA, USA, E-mail:rmellors@geology.sdsu.edu
⁽²⁾ Scripps Institution of Oceanography, University of California San Diego, San Diego, CA, USA, E-mail:dsandwell@ucsd.edu

Abstract. ALOS PALSAR data is used to construct an interferogram in the Tien Shan of Kyrgyzstan. This region is challenging for interferometry due to high topographic variations, frequent snowfall, and vegetation. The M_w 5.8 Dec. 26 Kochkorka, Kyrgyzstan earthquake, which damaged several hundred houses, is chosen as a test target. An interferogram from 11 Nov 2006 to 19 February 2007 is generated. Correlation over the entire interferogram is excellent despite snow cover over much of the region. A possible signal (less than 3 cm line-of-sight range change) is observed at the location of the fault plane, as defined by aftershocks. Modeling of this signal indicates that the fault plane must be at least 12 km deep at the top and likely includes a component of strike-slip motion. InSAR processing was conducted using the SIOSAR package.

Keywords: ALOS, interferometry, Tien Shan, earthquakes

1. INTRODUCTION

The northern Tien Shan of Central Asia is an area of active mid-continent deformation. Although far from a plate boundary, this region has experienced 5 earthquakes larger than magnitude 7 in the past century and includes one event that may be as large as M_w 8.0. Previous studies based on GPS measurements indicate on the order of 23 mm/yr of shortening across the entire Tien Shan and up to 15 mm/year in the northern Tien Shan (Figure 1) [1,2]. The strain measured by geodesy matches the expected seismic moment release rate [3], at least to first order, suggesting that geodetic rates can be considered a proxy for accumulation rates of stress for seismic hazard estimation.

This tectonic shortening appears to be distributed evenly across the entire range, at least at the resolution of the GPS network. A study of fault slip rates based on paleoseismic and geologic data [4] suggests that most slip occurs on a few key faults spaced roughly 30-50 km apart within the Tien Shan, indicating a block-like pattern of deformation with little internal deformation within each block. Seismicity maps of the region do not show clear block boundaries but indicate broad belts of seismicity which suggest more distributed mode of deformation. Published geological maps also show a dense set of thrust faults throughout the region although it is not clear if all are active. Efforts [5] have been made to define and model the deformation using block models but modeled fault slip

rates are dependant on the choice of block boundaries. Although the overall fit to observed signals is reasonable, significant discrepancies between model rates and estimated geologic rates remain (notably along the Talas Ferghana fault).

A clear understanding of the expected fault slip along each active fault is essential in assessing regional seismic hazard. A model which allows the 15 mm/slip to be distributed across many small blocks means a lower recurrence rate at any one fault and hence a lower risk for any particular fault. This is critical for assessing risk along the northern boundary faults near the major population centers of Bishkek and Almaty. As an example, one study [4] indicates that the expected slip rate at the Issyk Ata fault next to the city of Bishkek (a population of over 1 million) might be as high as 5 mm/year. A model with more distributed slip could reduce this to 2 mm/year (or less). Since this fault has not ruptured in at least 200 hundred years (and likely more), the difference in the two models creates a significant variation in the size of the potential earthquake.

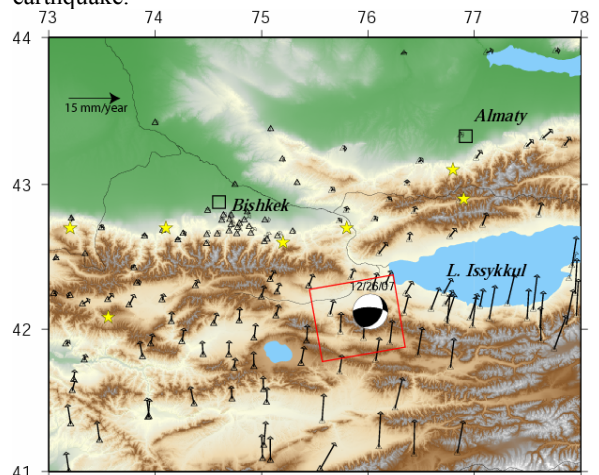


Figure 1. Map of northern Tien Shan. Arrows show showing crustal motion vectors measured by GPS. Yellow stars are historical large (> M 6.5) earthquakes and cities (> 1 million) are denoted by squares. The red square shows area of the ALOS PALSAR images and the focal mechanism shows the position of the 2006 Kochkorka earthquake.

Higher resolution using GPS is possible over small areas but impractical over the entire Tien Shan. Interferometric synthetic aperture radar may provide a means to make detailed spatial measurements and hence can assist in identifying block boundaries and defining seismic hazard. Previous efforts using C band radar (ERS and Envisat) encountered significant difficulties due to temporal decorrelation due to vegetation and snow. Here we present initial results of interferometry in the Tien Shan using ALOS L band radar.

We look at the Dec. 26, 2006, Kochkorka earthquake using ALOS PALSAR interferometry. The ALOS results are compared with results from seismic data and simple modeling. The Kochkorka (M_w 5.8) earthquake destroyed or severely damaged 400 houses as well as power and communication lines in the region [6].

2. Data

2.1 Seismic and geologic data.

The earthquake was well recorded by a local broadband seismic network as well as global stations. The local network also recorded numerous aftershocks, which we relocated using the algorithm of [7]. The global focal mechanism [8] indicated a thrust mechanism with a component of strike-slip. The aftershocks suggest a south-dipping thrust fault striking NNE and dipping at an angle of 35-45° (Figure 2). Well-constrained aftershocks ranged from about 6 km to 26 km in depth. A previous large earthquake in the region possessed a similar mechanism and aftershock depth distribution [9]. No known surface rupture has been mapped as far as we know but this fault orientation is consistent with a continuation of the South Kochkorka thrust fault [4].

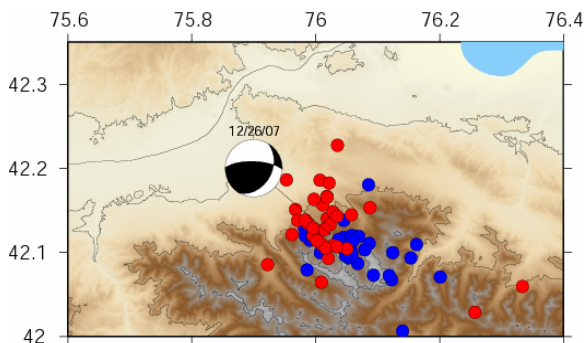


Figure 2. Focal mechanism of main shock (Centroid moment tensor [8]) and locations of aftershocks as located by a local seismic network. Red circles represent hypocenters less than 10 km and blue circles represent hypocenters deeper than 10 km. The aftershocks indicate a fault plane dipping to the southeast, which matches the orientation of known faults in the area.

2.2 ALOS PALSAR interferometry.

Two ALOS images (frame 830 path 522, ascending) acquired on 11 Nov. 2006 and on 19 February 2007 span the time and area of the earthquake with a perpendicular baseline of 95 m. An interferogram was calculated using the SIOSAR software with unwrapping performed using an algorithm from [10]. Elevation corrections were estimated using the SRTM DEM. Missing pixels in the DEM in areas of high terrain gradients were interpolated to reduce artifacts and a planar trend was removed from the unwrapped interferogram. The SIOSAR package was used with modifications made to read ALOS PALSAR data (see appendix A).

The interferogram possessed good coherence over most of the scene, even though much of the area was likely covered by at least a thin layer of snow at the time of the individual frames, as all of the region covered by the frame is in excess of 2000 m elevation and includes peaks as high as 5000 m. The surface is rocky and rugged.

The first, somewhat surprising, observation was that a clear signal was not observed despite good correlation over the area of the earthquake (Figure 3A). The lack of a clear signal (< 5 cm line of sight displacement) indicates that either the majority of the slip was deep or resolved poorly by the look angle of the radar. After removal of the trend, a subtle signal was observed at the location of the earthquake and aftershocks. A correlation was noted between topography and phase at the location of the earthquake. The source of this correlation is not clear and may be due to errors in baseline calculation, a layered atmosphere, or other effects. As the high topography in this region is largely a product of movement on thrust faults, some correlation between the surface deformation and topography is also expected.

To remove any residual topographic effect, an additional correction factor was estimated based on the observed correlation between phase and topography and applied to the interferogram (Figure 3B). The possible earthquake signal was reduced in amplitude but was not eliminated completely. This correction may, in view of later modeling results, overcompensate and eliminate part of the deformation signal. Given the possibility of systematic bias we cannot be certain that the signal is definitely due to surface deformation, especially with a single interferogram but the interferogram does place an upper limit on the maximum deformation. In turn, this provides important constraints on the depth and slip of the earthquake, which we explore with simple modeling.

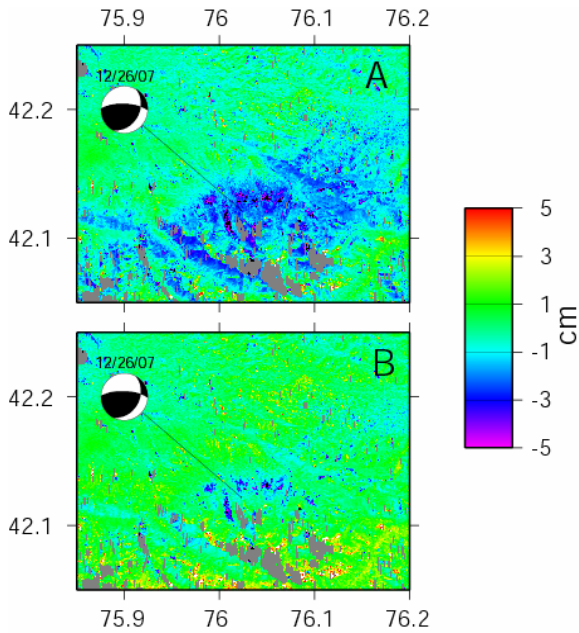


Figure 3. Interferogram of area shown in Figure 1 as originally generated (A) and with and additional elevation correction (B). Scale in cm and refers to line-of-sight range change.

2.3. Modeling

We use an analytic solution [11] to model the expected deformation based on parameters estimated from seismic data (Table 1; Figure 4). The focal mechanism derived from global data is used as a starting point. The dip was set at 40 degrees, based on the focal mechanism and aftershock depths. The length and width of the fault were based on the aftershock distribution and total moment release. Several models with varying rake and depth of slip were tested. A pure thrust mechanism greatly overestimated the observed deformation. Only by including a significant amount of strike-slip motion and by reducing the moment release (from M_w 5.8 to M_w 5.3) could the seismic data be reconciled with the InSAR observations.

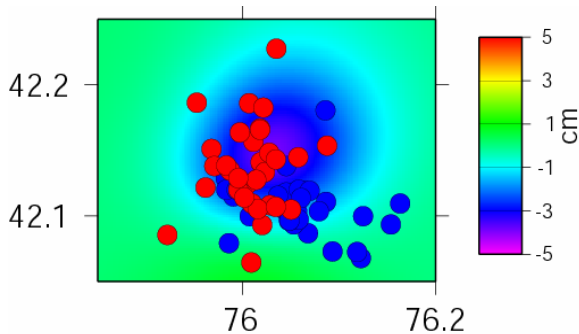


Figure 4. One possible model of line-of-sight surface deformation using the parameters in Table 1. Aftershocks as noted in Figure 1.

Table 1. Model parameters

Latitude, longitude	42.1, 75.975
Strike, dip, and slip	30°, 40°, 34°
Depth (top)	8 km
Length (horizontal)	8 km
Width	8 km
Slip	1.2 m
Moment, M_w	1.0×10^{24} , M_w 5.3

3. DISCUSSION AND CONCLUSIONS

The interferogram calculated using the ALOS PALSAR data demonstrates that the L-band data is useful for interferometry over this area. Our previous experience using C-band radar has been less successful and showed rapid temporal decorrelation even over the space of a few months. Although we do not have C-band data for the time period and area covered by this interferograms and cannot make a direct comparison, our experience with several years of C-band data suggests that the L-band shows significantly better correlation and hence may be useful in detecting long-term tectonic motion.

The possible detection of the Kochkorka earthquake shows that useful constraints can be placed on even moderate size earthquakes and that the combination of seismic data and satellite radar is a powerful and inexpensive method to monitor fault movement in this region. Further efforts will be made to calculate additional interferograms.

4.0 APPENDIX: SOFTWARE AND PROCESSING

The INSAR processing code was a modified version of the SIOSAR package developed at the Scripps Institute of Oceanography [12]. Additional software to read ALOS data, calculate baselines, merge images, and interpolate data is available at [13] and [14]. The code will work with either the freely available SIOSAR or ROIPAC processing packages.

Acknowledgements

This research is conducted under the agreement of JAXA Research Announcement titled ‘ALOS PALSAR Interferometry in the Tien Shan’ (JAXA-152) and with support from CRDF project KYG1-2879-BI-07 to R. Mellors. The Alaska SAR facility provided assistance with data.

References

- [1] Abdrakhmatov, K.E., S.A. Aldazhanov, B.H. Hager, M.W. Hamburger, T.A. Herring, K.B. Kalabaev, V.I. Makarov, P. Molnar, S.V. Panasyuk, M.T. Prilepin, R.E. Reilinger, I.S. Sadybakasov, B.J. Souter, Yu.A. Trapeznikov, V.E. Tsurkov and A.V. Zubovich, Relatively recent construction of the Tian Shan inferred

from GPS measurements of present-day crustal deformation rates, *Nature* 384 (1996), pp. 450–453.

[2] Zubovich, A. V., Y.A. Trapeznikov, V.D. Bragin, O.I. Mosienko, G.G. Shchelochkov, A.K. Rybin and V.Yu. Batalev, Deformation field, Earth's crust deep structure, and spatial seismicity distribution in the Tien Shan, *Russian Geology and Geophysics* 42 (2001), pp. 1634–1640.

[3] Molnar, P. and S. Ghose, Seismic moments of major earthquakes and the rate of shortening across the Tien Shan, *Geophys. Res. Lett.*, 27, 2377-2380, 2000.

[4] Thompson, S. C., R. J. Weldon, C. M. Rubin, K. Abdrakmatov, P. Molnar, and G. W. Berger, Late Quaternary slip rates across the central Tien Shan, Kyrgyzstan, Central Asia, *J. Geophys. Res.*, 107, (B9), 2203, doi:10.1029/2001JB000596, 2002.

[5] Meade, B. J., and B. H. Hager, The current distribution of deformation in the Western Tien Shan from block models constrained by geodetic data, *Geologia i Geofizika*, 42, 1622-1633, 2001.

[6] <http://www.ifrc.org/docs/appeals/06/MDRKG001.pdf>

[7] Pavlis, G. L., F. Vernon, D. Harvey, and D. Quinlan (2004). The generalized earthquake-location (GENLOC) package: an earthquake-location library. *Computers & Geosciences*, 30, 1079-1091.

[8] <http://www.globalcmt.org/>

[9] Mellors, R. J., F. L. Vernon, G. L. Pavlis, G. A. Abers, M. W. Hamburger, S. Ghose, and B. Iliasov, The Ms=7.3 Suusamy, Kyrgyzstan earthquake: 1: Constraints on fault geometry and source parameters based on aftershocks and body-wave modeling, *Bulletin of the Seismological Society of America*, 87,11-22, 1997.

[10] Ghiglia, D. C. and M. D. Pritt, Two-Dimensional phase unwrapping: Theory, Algorithms, and Software, John Wiley and Sons, 493 p., 1998.

[11] Wang, R., F.L. Martini and F. Roth, Computation of deformation induced earthquakes in a multi-layered elastic crust – FORTRAN programs EDGRN/EDCMP, *Comput. Geosci.*, 29, 195-207, 2003.

[12] http://igpphelp.ucsd.edu/admin/IGPP_software.html

[13] <http://www-rohan.sdsu.edu/~rmellors/>

[14] <http://roipac.org/>